Nanofabrication of surface-enhanced Raman scattering device by an integrated block-copolymer and nanoimprint lithography method

E. L. Yang[a]
Sandia National Laboratories, Livermore, California 94550

C. C. Liu
Department of Chemical and Biological Engineering, University of Wisconsin Madison, Wisconsin 53706

C. Y. P. Yang and C. A. Steinhaus
Sandia National Laboratories, Livermore, California 94550

P. F. Nealey
Department of Chemical and Biological Engineering, University of Wisconsin Madison, Wisconsin 53706

J. L. Skinner
Sandia National Laboratories, Livermore, California 94550

(Received 12 July 2010; accepted 30 August 2010; published 1 December 2010)

The integration of block-copolymers (BCPs) and nanoimprint lithography (NIL) presents a novel and cost-effective approach to achieving nanoscale patterning capabilities. The authors demonstrate the fabrication of a surface-enhanced Raman scattering device using templates created by the BCP-NIL integrated method. The method utilizes a poly(styrene-*block*-methyl methacrylate) cylindrical-forming diblock-copolymer as a masking material to create a Si template, which is then used to perform a thermal imprint of a poly(methyl methacrylate) (PMMA) layer on a Si substrate. Au with a Cr adhesion layer was evaporated onto the patterned PMMA and the subsequent lift-off resulted in an array of nanodots. Raman spectra collected for samples of R6G on Si substrates with and without patterned nanodots showed enhancement of peak intensities due to the presence of the nanodot array. The demonstrated BCP-NIL fabrication method shows promise for cost-effective nanoscale fabrication of plasmonic and nanoelectronic devices. © *2010 American Vacuum Society.* [DOI: 10.1116/1.3501341]

I. INTRODUCTION

Innovative solutions are necessary in order to continue satisfying Moore's law in the field of microelectronics.[1] Standard photolithography techniques are no longer viable as a solution to the reduction of feature sizes due to physical limits of diffraction.[2] Electron beam (e-beam) lithography was originally the elected solution due to its sub-50 nm single exposure resolution capability, but has fundamental limitations due to the serial write method. However, serial write methods can be economical and manufacturable when used to make masks or templates that pattern substrates in a parallel fashion, such as nanoimprint lithography (NIL). The need for nanolithography (sub-100 nm) techniques has led to novel solutions, with some advancing beyond the standard photolithography paradigm.

These next-generation lithography solutions include shorter-wavelength lithography approaches (e.g., extreme ultraviolet lithography and x-ray lithography), biological or chemically induced self-assembled lithography [e.g., DNA based templating and block-copolymers (BCPs)], and alternative lithographic techniques (e.g., nanoimprint lithography and interference lithography).[3] Of these solutions, nanoimprint is considered a promising avenue, boasting 5 nm linewidth and 14 nm pitch feature capability as well as high throughput capability due to its simple pattern transfer technique.[4] Some industrial companies, such as makers of magnetic and optical media, are investigating a combination of e-beam lithography (for imprint template writing) and nanoimprint lithography (for high throughput fabrication) as the most promising solution.[5]

E-beam lithography used to pattern imprint templates, however, has limitations. Although the intrinsic resolution of writing is around 5 nm, pattern transfer from the resist to the substrate generally leads to more realistic feature sizes of 10 nm with minimum pitch around 30 nm.[6] In addition, e-beam lithography is a slow, serial patterning process and is expensive due to complex machinery.

In this article, we present an integrated BCP and NIL method as a manufacturable solution for nanoscale lithography. Block-copolymers present a self-assembly based approach toward rapid nanoimprint template production with no need for complex machinery. Typically, the periodic domains formed by phase separation of two or more dissimilar polymers are on the order of 5–50 nm in size.[7] The morphology of the nanodomains depends on the volume fractions of the two blocks. Block-copolymers for nanolithography is an emerging field, and literature already demonstrates feasible applications such as biomolecular arrays and CMOS devices.[8–10]

[a]Electronic mail: elai@sandia.gov

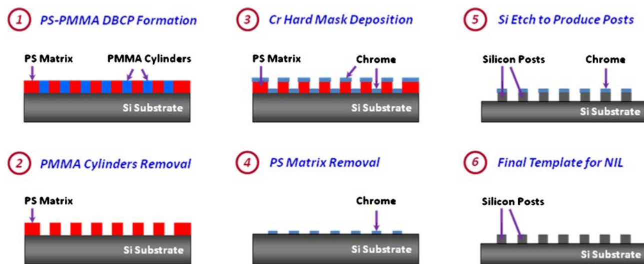

FIG. 1. (Color online) Fabrication procedure of silicon template by diblock-copolymer self-assembly.

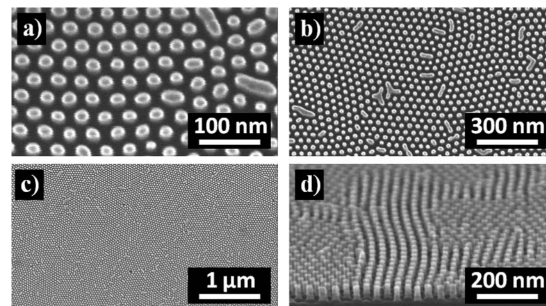

FIG. 2. [(a)–(c)] Top view and (d) tilted view SEM images of silicon template made by diblock-copolymer self-assembly.

Using our integrated BCP-NIL process, we demonstrate the fabrication of a surface-enhanced Raman spectroscopy (SERS) device. A nanoimprint template was fabricated by using the self-assembly of a diblock-copolymer [poly(styrene-*block*-methyl methacrylate) (PS-*b*-PMMA)] to form an etching mask for the creation of posts on a silicon wafer. This template in turn was used in a nanoimprint pattern transfer to create a resist layer with holes. Metal deposition and lift-off resulted in an array of Au nanodots measuring 20 nm in diameter. These nanodots were subsequently shown to produce an enhancement in the Raman scattering signature of Rhodamine 6G (R6G) interrogation molecules.

To the authors' knowledge, only one group has demonstrated a similar integrated approach of using block-copolymers to create a silicon template for nanoimprinting. They were successful in fabricating 30 nm pitch magnetic dot arrays for the purpose of magnetic media.[11] An analogous idea was carried out in another group by employing the self-assembly of anodic aluminum oxide templates for nanoimprint lithography.[12] Other than these two groups, the only other related work found involved using nanoimprint as a physical prepattern tool for the self-assembly of diblock-copolymers.[13,14] The work presented here is the first to apply the integrated BCP-NIL fabrication method to create a working device, namely, a SERS device.

II. FABRICATION

The fabrication procedure involves a series of two pattern transfers. First, a directed block-copolymer assembly is utilized to form an array of perpendicularly oriented PMMA cylinders in a PS matrix. This pattern is transferred to a silicon substrate via lift-off and plasma etching, resulting in an array of silicon posts. These posts are used in a second pattern transfer via nanoimprinting to a layer of resist. An array of holes is produced in the resist, and this pattern is used to fabricate the SERS device.

A. Diblock-copolymer template

The diblock-copolymer self-assembly uses thin films of PS-*b*-PMMA. The fabrication process is illustrated in Fig. 1. First, a hydroxyl-terminated random copolymer brush layer was deposited on a 4 in. silicon substrate. Then, a thin film (35 nm) of the block-copolymer (PS-*b*-PMMA) was spun onto the substrate and annealed under vacuum to initiate self-assembly. The result was hexagonal arrays of perpendicularly oriented PMMA cylinders in a PS matrix. The PMMA domains were then selectively removed with UV exposure and subsequent glacial acetic acid exposure. Details of this diblock-copolymer self-assembly process are described elsewhere.[15–18] Chromium (measuring 15 nm in thickness) was evaporated onto the exposed underlying Si and remaining PS matrix. Lift-off in a piranha solution removed the PS and left hexagonal arrays of Cr nanodots to serve as an etch mask for the subsequent dry plasma Si etch. An inductively coupled plasma reactive ion etch (using C_4F_8, SF_6, and Ar with a power of 60 W) was performed to transfer the pattern into the silicon substrate. The resulting silicon posts shown by the scanning electron images in Fig. 2 have dimensions of approximately 20 nm in diameter, 40 nm in pitch, and 44 nm in height. The sidewalls are approximately vertical and the rods are circular in cross section. The hexagonal patterns reside in larger "grains" and structural defects could be attributed to imperfections in the self-assembly process.

B. Nanoimprint lithography

The silicon template was then employed in a nanoimprint pattern transfer. The fabrication process is illustrated in Fig. 3. A diluted solution of PMMA was spun onto a separate 4 in. silicon wafer to a thickness of approximately 50 nm. A thermal imprint was performed at 200 °C and 400 psi for 5 min. Scanning electron microscopy (SEM) images of the im-

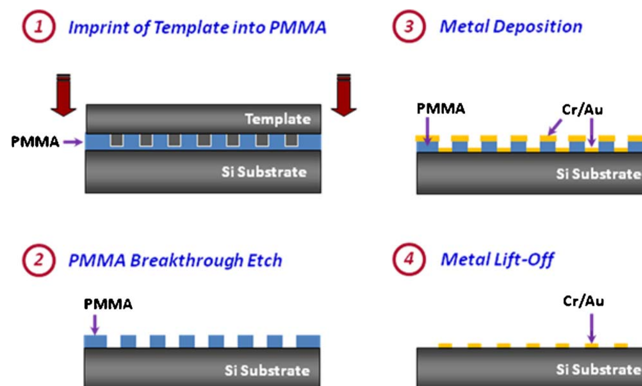

FIG. 3. (Color online) Fabrication procedure of SERS device by nanoimprint lithography.

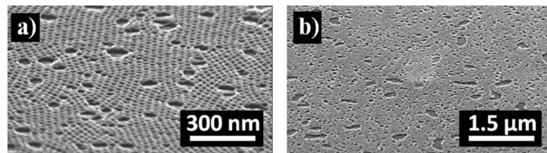

FIG. 4. Tilted view SEM images of PMMA imprint made by nanoimprint lithography.

printed PMMA resist are shown in Fig. 4. The small holes seen in the imprint are a result of successful pattern transfer. Larger voids were formed with nominal diameters of 150 nm. The origin of these larger voids are still not well understood and are speculated to be either gas bubbles originating from the dilution of the PMMA or areas of PMMA that delaminated during the pattern transfer step.

C. Surface-enhanced Raman spectroscopy device

After imprint, the residual PMMA layer at the bottom of the holes was removed by an oxygen plasma inductively coupled reactive ion etch [30 W rf power, 25 SCCM (denoted as standard cubic centimeter per minute at STP), of O_2 flow, and 5 mTorr chamber pressure]. Cr of 1 nm thickness was e-beam evaporated onto the imprinted substrate as an adhesion layer, followed by 5 nm of Au. Lift-off was then performed for 30 min in an ultrasonic bath to remove the unwanted PMMA and metal layers, leaving behind Au nanodots. It was found that removing 25 nm of the PMMA (half of the initial thickness) during the oxygen plasma etch provided the optimum conditions for a successful resist lift-off. If less than 25 nm of the initial PMMA thickness were etched, the residual PMMA layer from the imprint process was not removed completely. The evaporated metal would, therefore, not adhere to the substrate. If more than 25 nm of the initial PMMA thickness were removed, then lock-in would occur due to excessive sidewall deposition of the evaporated metal. Lift-off would then be unsuccessful in removing the PMMA. Metal thicknesses of 1 nm Cr and 5 nm Au proved to be the most optimal thicknesses for a successful lift-off.

Figure 5(a) presents a SEM image of the Cr/Au metal

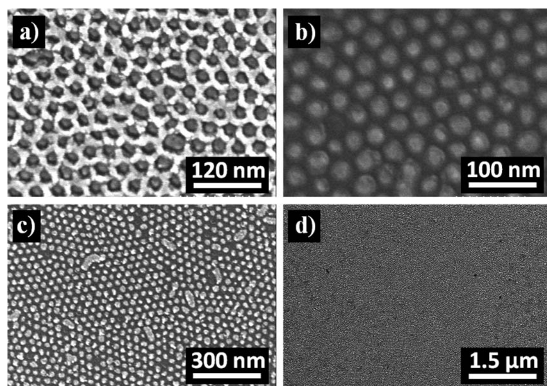

FIG. 5. Top down SEM images of Au nanodot SERS device (a) before lift-off and [(b)–(d)] after lift-off.

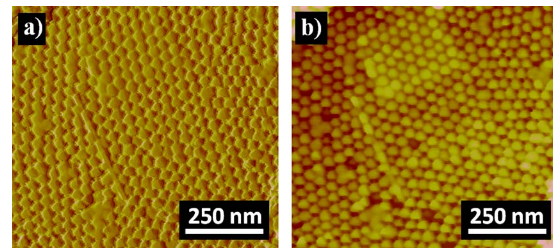

FIG. 6. (Color online) (a) Amplitude and (b) height AFM measurements of Au nanodot SERS device.

deposited onto the PMMA imprint pattern before lift-off. The metal dots (dark gray) are clearly visible inside the imprinted holes. It is apparent that some dimensionality and circularity have been lost during the nanoimprint pattern transfer process. The imprinted holes now measure 20–35 nm in diameter. After lift-off, Cr/Au nanodots remain on the surface of the silicon substrate. The dimensionality and circularity loss in these nanodots is transferred from the imprint pattern and could be seen in the SEM images in Figs. 5(b)–5(d). The metal nanodots measure 20–33 nm in diameter. Peanut shaped defects are due to the transfer of imperfections from the original block-copolymer assembly, while single dot voids are due to the failure of punching through the entire residual PMMA layer.

Atomic force microscopy (AFM) measurements were also taken on the Cr/Au nanodot sample. The height of the nanodots appears relatively uniform across the sample. These measurements are shown in Fig. 6.

III. RESULTS AND DISCUSSION

A. Surface-enhanced Raman scattering

Localized surface plasmon resonances are excited when light is incident upon metal nanoparticles, resulting in localized electric field oscillations.[19] Molecules adsorbed to these metal surfaces, and therefore residing within the vicinity of the electric fields, have been shown to exhibit enhanced Raman scattering due to both an increase in light absorption by the molecules as well as an increase in the resulting Raman scattering intensities.[20] This phenomenon is well known and was first discovered in the 1970s.[21,22]

When the incident light is near the plasmon resonance frequency of a particular metal material, the effect is more significant. Silver and gold have plasmon resonance frequencies in the visible region and, therefore, are commonly used in performing SERS experiments.[19] The effect can be further enhanced by roughening the metal surfaces or creating shapes with sharp edges or corners to further localize the electric fields, creating "hot spots."[23] Furthermore, placing the particles in close proximity to one another could also enhance the effect by creating collective electric field oscillations.[24,25]

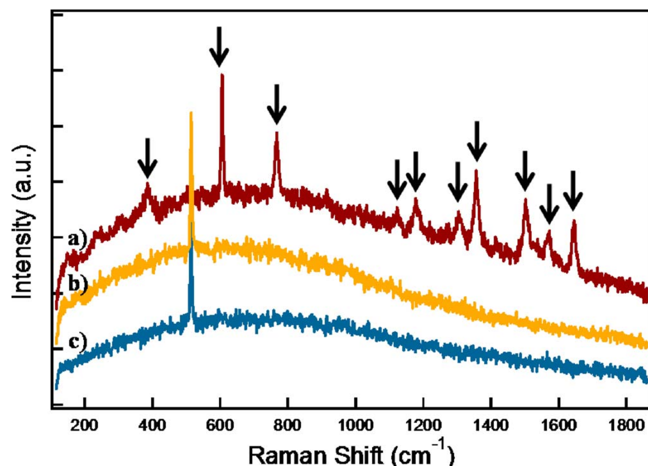

FIG. 7. (Color online) Raman scattering plots of R6G on (a) device chip—patterned section, (b) control chip—bare silicon, and (c) device chip—bare silicon section. Black arrows denote R6G scattering peaks.

B. Experimental setup

R6G was chosen as the interrogation molecule for testing the SERS device due to its richly featured and recognizable Raman scattering spectrum.[26] One droplet (approximately 0.05 ml) of $1\times10^5 M$ R6G in methanol was placed on a 1×1 cm^2 device chip (cleaved from the original wafer) and allowed to air dry. The 532 nm line of a neodymium:yttrium aluminum garnet laser was used as the excitation source. Gold was chosen as the plasmonic material due to its well known resonance in the midvisible region and was, therefore, well matched to the excitation wavelength.[19,20] The total power incident on the substrate surface was approximately 1 mW and the laser spot size was approximately 650 nm in diameter. The Raman scattering spectra were collected over 1 s collection times.

C. Raman scattering

The Raman scattering spectra in Fig. 7 indicate an enhancement of the R6G peaks in the presence of the Au nanodots. The spectra were collected in three scenarios: (1) the laser spot was focused on an area of the device chip where there are Au nanodots, (2) the laser spot was focused on a bare silicon area of the same device chip where there were no Au nanodots, and (3) the laser spot was focused on a control chip of bare silicon with no Au nanodots.

In scenario 1, many peaks are visible in the Raman scattering spectra. The peaks denoted by the arrows are associated with R6G and are clearly visible.[26] In scenarios 2 and 3, the same peaks are not discernible, suggesting enhanced Raman scattering in scenario 1. Furthermore, the 519 cm^{-1} peak is clearly visible on all three spectra and is associated with the Raman signature of the silicon substrate. In fact, the magnitude of the 519 cm^{-1} peak in the three scenarios is virtually unchanged, which supports the conclusion that the enhancement in the R6G peaks is indeed caused by the presence of the Cr/Au nanodots. Scenario 2 further supports the claim by ensuring that approximately the same number of R6G molecules resided in the interrogation areas, since the substrate used in scenarios 1 and 2 was the same substrate that was subjected to the same droplet of R6G solution. In total, approximately 15 measurements were done on independently located Au nanodots to verify the enhancement.

IV. CONCLUSIONS

In summary, the integration of diblock-copolymer self-assembly and nanoimprint lithography presents a more rapid and cost-effective approach to nanofabrication as compared to conventional e-beam template writing. The technique enables sub-50 nm feature pattern transfers. We have demonstrated the fabrication of a Cr/Au nanodot SERS device and confirmed the enhanced Raman scattering signals of R6G molecules adsorbed onto the device surface.

Initial results show varying defects and imperfections ensuing each pattern transfer step. Future work will focus on obtaining more ordered diblock-copolymer assemblies, improving imprint yield over larger areas, eliminating imprint voids, and retaining the dimensionality and fidelity of shapes. Also, the magnitude of enhancement of Raman scattering peaks could likely be improved by optimizing the size of the nanoparticles.

Our demonstrated BCP-NIL fabrication method shows promise for cost-effective nanoscale fabrication and could be adopted for potential applications in plasmonic and nanoelectronic devices.

ACKNOWLEDGMENTS

A portion of this work was supported by the Laboratory Directed Research and Development program at Sandia National Laboratories. Sandia is a multiprogram laboratory operated by Sandia Corporation, a Lockheed Martin Company, for the United States Department of Energy's National Nuclear Security Administration under Contract No. DE-AC04-94AL85000.

[1]G. E. Moore, Proc. SPIE **2438**, 2 (1995).
[2]M. J. Bowden, Stevens Alliance Technol. Manage. **8** (2004).
[3]R. Luttge, J. Phys. D **42**, 123001 (2009).
[4]M. D. Austin, H. Ge, W. Wu, M. Li, A. Yu, D. Wasserman, S. A. Lyon, and S. Y. Chou, Appl. Phys. Lett. **84**, 5299 (2004).
[5]B. Heidari and M. Beck, Proc. SPIE **6921**, 692103 (2008).
[6]C. Vieu, F. Carcenac, A. Pépin, Y. Chen, M. Mejias, A. Lebib, L. Manin-Ferlazoo, L. Couraud, and H. Launois, Appl. Surf. Sci. **164**, 111 (2000).
[7]H.-C. Kim, S.-M. Park, and W. D. Hinsberg, Chem. Rev. (Washington, D.C.) **110**, 146 (2010).
[8]J. P. Bearinger *et al.*, Langmuir **25**, 1238 (2009).
[9]L. W. Chang, M. A. Caldwell, and H. S. P. Wong, Proc. SPIE **6921**, 69212M (2008).
[10]J. Y. Cheng, D. P. Sanders, H. C. Kim, and L. K. Sundberg, Proc. SPIE **6921**, 692127 (2008).
[11]N. Kihara, H. Hieda, and K. Naito, Proc. SPIE **6921**, 692126 (2008).
[12]K. Liu, S. Fournier-Bidoz, G. A. Ozin, and I. Manners, Chem. Mater. **21**, 1781 (2009).
[13]H.-W. Li and W. T. S. Huck, Nano Lett. **4**, 1633 (2004).
[14]J. P. Lee, E. U. Kim, H. D. Koh, N. G. Kang, G. Y. Jung, and J. S. Lee, Nanotechnology **20**, 365301 (2009).
[15]R. Ruiz, H. Kang, F. A. Detcheverry, E. Dobisz, D. S. Kercher, T. R. Albrecht, J. J. de Pablo, and P. F. Nealey, Science **321**, 936 (2008).
[16]H. J. Park, M.-G. Kang, and L. J. Guo, ACS Nano **3**, 2601 (2009).
[17]S.-M. Park, G. S. W. Craig, C.-C. Liu, Y.-H. La, N. J. Ferrier, and P. F.

Nealey, Macromolecules **41**, 9118 (2008).
[18]A. J. Hong, C.-C. Liu, Y. Wang, J. Kim, F. Xiu, S. Ji, J. Zou, P. F. Nealey, and K. L. Wang, Nano Lett. **10**, 224 (2010).
[19]W. A. Murray and W. L. Barnes, Adv. Mater. **19**, 3771 (2007).
[20]K. Okamoto, I. Niki, A. Shvartser, Y. Narukawa, T. Mukai, and A. Scherer, Nature Mater. **3**, 601 (2004).
[21]M. Fleischmann, P. J. Hendra, and A. J. McQuillan, Chem. Phys. Lett. **26**, 163 (1974).
[22]D. L. Jeanmaire and R. P. Van Duyne, J. Electroanal. Chem. **84**, 1 (1977).
[23]M. J. Mulvihill, X. Y. Ling, J. Henzie, and P. Yang, J. Am. Chem. Soc. **132**, 268 (2010).
[24]M. A. Noginov, M. Vondrova, S. N. Williams, M. Bahoura, V. I. Gavrilenko, S. M. Black, V. P. Drachev, V. M. Shalaev, and A. Sykes, J. Opt. A, Pure Appl. Opt. **7**, S219 (2005).
[25]J. Chen, T. Martensson, K. A. Dick, K. Deppert, H. Q. Xu, L. Samuelson, and H. Xu, Nanotechnology **19**, 275712 (2008).
[26]A. M. Michaels, M. Nirmal, and L. E. Brus, J. Am. Chem. Soc. **121**, 9932 (1999).